1.0 OBJECTIVE

The objective of this work was to develop a stable non-iron Fischer-Tropsch catalyst, more selective to distillate fuels and with lower light ends production relative to Sasol's Arge precipitated iron catalyst.

2.0 INTRODUCTION

This project was conducted at the UOP Des Plaines Technical Center between 1/1/84 and 2/28/89 under Contract DE-AC22-84PC70023 from the Department of Energy.

As an introduction, first, the basic objective of the research program will be summarized, followed by a discussion of the relevant background work, and a discussion of the research approach. Finally, the project team will be described.

2.1 Problem Statement

Fischer-Tropsch synthesis products, with current catalyst systems, obey the Anderson-Schulz-Flory polymerization law by which the probability of chain growth is independent of carbon number. This polymerization law imposes strict maxima on the selectivity toward desirable liquid fuel products. Accordingly, light olefins have to be oligomerized and Fischer-Tropsch wax has to be hydrocracked in order to increase the overall yield to liquid fuels. Light paraffins are more difficult to upgrade: methane and ethane may be recycled back to a steam reforming unit to make more synthesis gas with significant loss to carbon oxides, while propane and butane may be sold as LPG. There is a great incentive to develop catalysts by which the overall yield to liquid fuels will be

enhanced. This objective can be achieved by developing a non-Anderson-Schulz-Flory Fischer-Tropsch catalyst that may provide a hydrocarbon cutoff at a carbon number of about 20, or by developing an Anderson-Schulz-Flory Fischer-Tropsch catalyst with minimal selectivity to light ends.

The research work summarized here attempted to achieve this objective by elucidating the relation between catalytic properties and the function of ruthenium Fischer-Tropsch catalysts. Ruthenium was chosen because of its higher specific activity relative to cobalt. Elucidating the relationship between the properties and function of Fischer-Tropsch catalysts holds the key to the development of selective catalysts. Most catalyst development work in the Fischer-Tropsch synthesis area, however, has been conducted in a semi-empirical fashion with minimal knowledge about the relationship between catalyst properties and function, specifically because:

i. a satisfactory Fischer-Tropsch catalyst data base under commercial-type operating conditions is not yet available,

ii. advanced catalyst preparation techniques have not been fully explored for precise catalyst design,

iii. advanced catalyst characterization techniques have not been satisfactorily utilized to substantiate catalyst improvements.

The ruthenium catalytic properties that were investigated here were particle size, metal-support interaction, ruthenium electronic state, and local coordination environment. An advanced catalyst preparation technique, which involved reverse micelles, was utilized to control ruthenium particle size and to ensure optimal interaction between ruthenium and the modifier atoms in the

finished catalyst. Advanced techniques such as STEM (scanning transmission electron microscopy), EXAFS (extended x-ray absorption fine structure), HRMS (high resolution mass spectrometry), NMR (nuclear magnetic resonance spectroscopy), and CO FTIR (CO Fourier transform infrared spectroscopy), along with more common techniques such as XPS (x-ray photoelectron spectroscopy), DSC (differential scanning calorimetry), TGA (thermogravimetric analysis), fluorescence and gas adsorption techniques were utilized in order to characterize fresh and used catalytic properties and to substantiate catalyst improvements that have been achieved. Most aspects of the ruthenium Fischer-Tropsch catalyst functions were monitored, including activity, selectivity, stability and the coking tendency.

2.2 Background Work

The relevant background work is described in five sections. First, the Fischer-Tropsch reaction mechanism is described, followed by discussion of the performance of state-of-the-art Fischer-Tropsch catalysts, review of literature reports of hydrocarbon cutoff, and review of particle size effects with ruthenium Fischer-Tropsch catalysts. Finally, principles of micelle formation are presented.

2.2.1 Fischer-Tropsch Synthesis Reaction Mechanism

2.2.1.1 Dissociative Chemisorption of CO

The first step in Fischer-Tropsch synthesis is the dissociative chemisorption of CO. CO dissociation requires several adjacent vacant metal atom sites. This large ensemble requirement probably makes the reaction structure sensitive [1]. For example, the probability of finding an ensemble of vacant metal atom sites decreases with a decrease in the metal particle size; accordingly the turnover number decreases.

Several forms of adsorbed CO species have been identified on the surface of Fischer-Tropsch catalysts by infrared spectroscopy. In the order of decreasing CO stretching frequency by infrared spectroscopy, some of these are [2]:

1. Twin CO (2 CO molecules bonded to a single metal atom)

2. Linear CO on cationic site

3. Linear CO on neutral metal surface (bonded to a single metal atom)

4. Bridged CO (bonded to more than one metal atom)

5. Tilted CO (bonded with its oxygen atom pointing toward the surface)

Here, the lower the frequence the higher is the weakening of the CO bond by the metal atom. The high frequency of CO on a cationic site appears to indicate that dissociation may not take place. One possible implication of this phenomenon is that the surface of working iron catalysts should contain a certain fraction of zero valent metal sites despite the presence of bulk oxide and carbide phases.

The coexistence of a small number of Fe^{0} sites with Fe^{n+} sites has been shown in the case of an alkali-promoted fused iron catalyst subjected to $5H_2/1CO$ at 1 atm, 200°C, by *in situ* laser Raman spectroscopy [3].

For unpromoted metal surfaces CO dissociation may occur via a bridged species [2]. In catalysts promoted with oxophilic agents, like potassium, CO dissociation may proceed via the tilted CO species caused by a favorable interaction between the oxygen in CO and this oxophilic promoter [2]. This effect is shown in Figure 2-1.

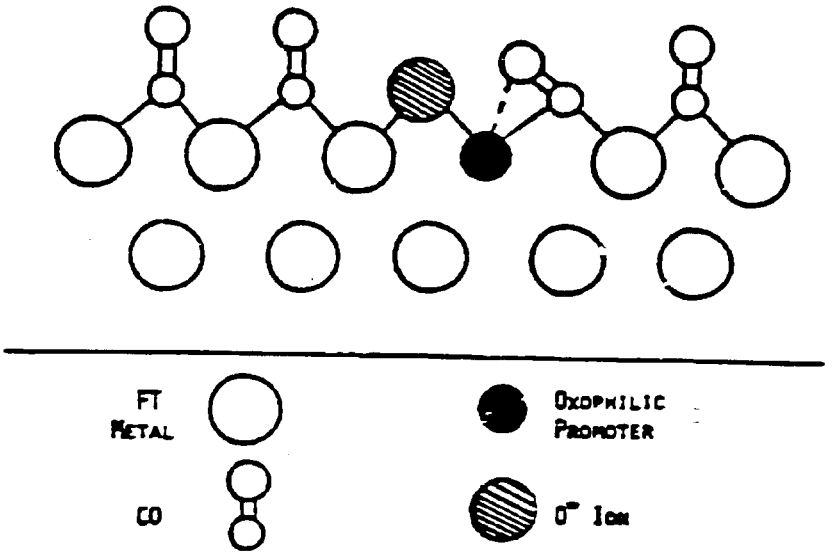

Figure 2-1. Effect of the Oxophilic Promoter on CO Chemisorption in Fischer-Tropsch Synthesis [2]

Not all Group VIII metals can dissociatively chemisorb CO. The calculated heat of dissociative adsorption at room temperature is highest on Fe, is lower with Co and Ni, is zero with Ru, is slightly negative with Os, Rh, Pd and Ir, and is quite negative with Pt [2]. Some of the transition metals like Mo and W with larger d-band vacancies have very favorable thermodynamics for dissociative CO chemisorption. However, these elements are not good Fischer-Tropsch catalysts, because they form excessively strong bonds with C and O [1,2].

The metal-carbon bond has to be of intermediate strength for a good Fischer-Tropsch catalyst; strong enough to favor CO dissociation, yet not too stable to prevent subsequent hydrogenation to methyl and methylene species. A very strong metal-carbon bond may then imply either relatively low activity or rapid deactivation.

One way of explaining the higher Fischer-Tropsch activity of ruthenium relative to iron then would be via comparison of the metal-carbon bond strength, which is larger for iron (calculated based on heat of formation of iron carbide [1] and graphite [4]) than for ruthenium [1]: 167 kcal/mole vs. 151 kcal/mole.

Similarly, the metal-oxygen bond also has to be of intermediate strength; strong enough to favor CO dissociation, yet not too stable to prevent reduction by H_2 to the lower oxidation state. It is important to note that the $H_2O:H_2$ ratio required to form the oxide decreases dramatically from Ru (7.1×10^9) to Co (7.6×10^1) and then finally to Fe (5.5×10^{-2}) [5]. Since Fischer-Tropsch activity also decreases from Ru to Co and then to Fe, an apparent inverse correlation exists between ease of oxidation under Fischer-Tropsch synthesis conditions and Fischer-Tropsch activity.

It appears that on ruthenium, CO dissociation is the most likely step for rate control, based on high CO surface coverages measured under reaction conditions. It has been reported, for instance, that carbonaceous deposits over Ru/SiO_2 could be hydrogenated at a rate considerably in excess of steady-state synthesis rates. Over iron, on the other hand, hydrogenation may be the rate determining step [6]. The C/H_2 reaction has been reported to be significantly slower on Fe relative to on Ru [7]. A slow CO dissociation step is consistent with the relatively weak nature of the Ru-C and Ru-O bonds. On the other hand, the relatively stable nature of the Fe-C and Fe-O bonds would explain both the ease of CO dissociation and the difficulty of hydrogenating the carbon to methyl and methylene species and the difficulty of hydrogenating the oxygen to form water.

2.2.1.2 Carbon Species in/on Working Fischer-Tropsch Catalysts

The carbon that results from CO dissociation either remains on the surface or diffuses inside the catalyst metal particles.

2.2.1.2.1 Reaction Intermediate Carbon

The carbon remaining on the surface of ruthenium catalysts and which participates directly in the formation of hydrocarbons has been identified by kinetic studies involving isotopically labeled species [8-11]. This primary reaction intermediate has been named as α-carbon by the group of A. Bell [11]. This carbon occupies no more than 2-7% of the ruthenium surface and may be bonded to the ruthenium metal with one or more bonds. This carbon is subsequently hydrogenated on the metal surface to form methyl ($M-CH_3$), methylene ($M=CH_2$) and methyne ($M\equiv CH$) type species which later form the hydrocarbons.

Reaction intermediate carbon on iron catalysts has also been identified by Mössbauer spectroscopy as a quadrupole doublet with an isomer shift = 0.0 and a quadrupole shift of 0.4 mm/sec [7].

2.2.1.2.2 Less Active Form of Carbon

A second form of carbon which does not directly participate in the formation of hydrocarbons, but which accumulates on the surface of ruthenium catalysts during Fischer-Tropsch synthesis has, also been identified by kinetic studies involving isotopically-labeled species. It was named as β-carbon by the group of A. Bell [11]. β-carbon is formed from α-carbon and contains hydrogen, at a ratio of 1.8-2.4 H:C. The β-carbon observed by the group of A. Bell is believed to be hydrocarbon like and closely resembles the alkyl chains observed by *in situ* infrared spectroscopy measurements by the group of K. Tamaru [12,13].

In the experiments conducted by the group of A. Bell, although β-carbon occupied no more than 13% of the ruthenium surface, it appeared to contain enough carbon to correspond to several monolayers. It is, therefore, suggested that alkyl chains in β-carbon stick out from the metal surface in a similar fashion to filamentous carbon observed with Ni, Fe, and Ru catalysts [7,14-18].

β-Carbon does not directly participate in the synthesis of hydrocarbons. However, it has been observed that when α-type carbon is depleted, β-type carbon can supply methyl-type C_1 intermediates to α-type carbon [12].

2.2.1.2.3 Poison Carbon

It appears that there is another form of carbon which leads directly to catalyst deactivation. This carbon may be formed by dehydrogenation of β-carbon. K. Tamaru *et al.* discusses that, under Fischer-Tropsch synthesis conditions, dehydrogenation of β-type carbon is inhibited by the presence of a large amount of adsorbed CO [12]. Dehydrogenation of β-carbon will require vacant sites for adsorption of product hydrogen and product coke, and the number of these sites will be minimal in the presence of adsorbed CO. It is interesting to note that during Mobil's work [19,20] it was repetitively observed that temporary replacement of synthesis gas by N_2 in the slurry reactor resulted in an irreversible loss of catalytic activity by the precipitated iron catalyst. Mobil's result is consistent with a deactivation phenomenon that involves dehydrogenation of β-type carbon that deposits coke on the bare surface when CO is removed from the gas phase.

Not much work has been done in chemical and physical characterization of the carbon which leads eventually to catalyst deactivation. Nevertheless, it may be speculated that coke will form by extensive dehydrogenation of β-carbon. Dehydrogenated carbon may undergo cyclization, followed by polymerization

reactions to deposit on the catalyst surface, as polynuclear aromatic compounds, which are the precursors to graphitic coke.

Graphitic carbon on iron catalysts has been identified both by its ESCA C1s binding energy of 284.7-285.0 eV and by the fine structure of its Auger signal [21].

It now appears that poison carbon on the surface of a Fischer-Tropsch catalyst can be both in the form of graphitic overlayers and in the form of filamentous carbon.

R. T. K. Baker's group at Exxon has postulated a mechanism for the growth of filamentous carbon from the catalyzed decomposition of acetylene, which depends on diffusion of carbon through the metal particle from the hotter leading face on which carbon deposits to the cooler trailing faces at which carbon is deposited from solution [7,14,15]. Carbon remaining at the leading particle surface migrates around the particle to constitute the wall of the filament. Growth ceases when the leading face of the particle is covered by a layer of carbon build-up as a consequence of rate control by the carbon diffusion process.

Similar carbon filaments, 0.01-0.2 μm in diameter, were observed to form by disproportionation of CO over iron, cobalt and nickel catalysts at 390°C [18].

It is conceivable that similar carbon filaments can occur during the exothermic Fischer-Tropsch synthesis reaction.

2.2.1.2.4 Bulk Carbide

The carbon that results from CO dissociation may diffuse inside the catalyst metal particles, and in the case of iron may form different phases of bulk carbide. The presence of bulk iron carbide is significant because iron carbide may act as the precursor for graphitic coke on iron as discussed by J. W. Geus [22].

2.2.1.3 Chain Growth and Termination

Chain growth is believed to occur by insertion of a methylene species to a metal-methyl bond [2]. Chain termination will occur by hydrogenation of the alkyl species to produce the paraffin or by β-hydrogen abstraction from the alkyl species to produce the corresponding α-olefin. The chain growth probability will increase with increased coverage and reactivity of the methylene species in the insertion reaction. The chain termination probability will increase with increasing hydrogenation plus dehydrogenation activity of the catalyst. Following this reasoning, chain termination by hydrogenation will be inhibited at low hydrogen partial pressures, and chain termination by dehydrogenation will be inhibited at high total pressure because of the unavailability of vacant sites for dehydrogenation product hydrogen.

2.2.1.4 Water Gas Shift Reaction

The water gas shift reaction may occur prior to the hydrocarbon synthesis reaction to generate hydrogen and carbon dioxide from water and carbon monoxide.

2.2.1.4.1 Water Gas Shift Catalysts

Water gas shift catalysts are traditionally classified as either high temperature (320-450°C) water gas shift catalysts, which are iron-based, or as low temperature (200-250°C) water gas shift catalysts, which are copper-based. Recently, a new type of water gas shift catalyst, cobalt-molybdenum-alkali-sulfur, has been reported to exhibit good activity both at high and low temperatures [23].

2.2.1.4.2 Water Gas Shift Reaction Mechanism

Two mechanisms have been commonly proposed for the water gas shift reaction [24]. The first one is the "associative mechanism" which involves an adsorbed formate intermediate. The proposed reaction sequence is:

i) dissociative adsorption of H_2O to give a surface hydroxyl and a surface hydrogen species

ii) molecular adsorption of CO to give a surface carbonyl species

iii) reaction of surface hydroxyl with surface carbonyl to give a surface formate species

iv) dehydrogenation of the surface formate to give CO_2 and surface hydrogen

v) desorption of CO_2 and molecular H_2.

Several metal oxide catalysts were evaluated for the water gas shift reaction at 357-447°C [24]. It was found that high water gas shift activity correlated with weak metal-oxygen bonds or with cations having low electronegativity. It was, therefore, proposed that the formate intermediate could form on basic oxides like MgO and ZnO. In acidic oxides, like Al_2O_3, strong metal-oxygen bonds caused rapid dehydration of the formate, apparently preventing the water gas shift reaction from proceeding. However, the same work also indicates that if the oxide is too basic then strong CO_2 adsorption will occur, inhibiting the kinetics of the water gas shift reaction.

The second mechanism is the "regenerative mechanism" in which the catalyst surface is successively oxidized by water adsorption on an oxygen vacancy to deposit surface hydrogen, followed by reduction with carbon monoxide which takes the oxygen away in the form of carbon dioxide and regenerates the oxygen vacancy [23]. For this kind of mechanism to be operative, the catalyst should have a cation which can change oxidation states rapidly. An example of a water gas shift catalyst which is believed to operate through the "regenerative mechanism" is magnetite (Fe_3O_4). The key feature in magnetite is apparently the presence of Fe^{+2} and Fe^{+3} ions which makes the regenerative mechanism possible [24].

2.2.1.4.3 Water Gas Shift Activity of Cobalt

Cobalt catalysts typically do not exhibit water gas shift activity during Fischer-Tropsch synthesis. However, it has been reported that some forms of cobalt, particularly at high temperatures and in the absence of H_2 in the feed, show water gas shift activity. For example, L. Wachowski *et al.* report that cobalt in perovskite-type oxides has high water gas shift activity at 347°C when cobalt is in divalent form, but not when it is in tetravalent form [25]. T. Khalacher *et al.* reports that cobalt oxide is not active in the water gas shift reaction unless at least 15% Fe_2O_3 is added [26]. The same authors also indicate that cobalt oxide promotion of iron-chromia catalysts significantly increases the rate of the water gas shift reaction at 340°C. There are several reports on the role of manganese in enhancing cobalt's water gas shift activity at similarly high temperatures [27-30]. The lowest temperature at which manganese-promoted cobalt was reported to exhibit considerable water gas shift activity during Fischer-Tropsch synthesis was at 250°C [28,30]. R. L. Varna argues that manganese addition to cobalt promotes the water gas shift reaction because it facilitates the dissociative adsorption of water [30]. Since water

is believed to compete for sites that adsorb hydrogen, a hydrogen deficiency is also proposed which may explain the olefinic nature of Fischer-Tropsch products obtained with manganese-promoted cobalt [30].

2.2.1.4.4 Water Gas Shift Activity of Ruthenium

Water gas shift activity at low temperatures was reported for ruthenium in Y-zeolite [31]. A redox couple involving two cationic forms of ruthenium (Ru^{+1} and Ru^{+2}) was proposed as the active site. K. C. Taylor *et al.* have evaluated alumina-supported ruthenium catalysts at 320-620°C with a feed simulating automotive exhaust gas (0.1% NO, 1% CO, 0.3% H_2, 10% CO_2, and 10% H_2O, 78.6% N_2) [32]. They reported oxidized Ru/Al_2O_3 to be an active water gas shift catalyst relative to reduced Ru/Al_2O_3, which was essentially inactive. D. Duprez *et al.*, who evaluated several supported group VIII metal catalysts for water gas shift reaction at 440°C in the absence of H_2 in the feed, reported that ruthenium was the most active element in this group [33].

2.2.2 State-of-the-Art Catalysts

The selectivity of Sasol's precipitated iron catalyst used in the Arge reactor is documented in the literature. This catalyst makes about 8.2% methane + ethane under the conditions expected to prevail in a new Arge-based refinery [34], (~225°C, 45 atm, 1.6-1.7 H_2:CO feed ratio). The overall light ends (C_1-C_4) selectivity has not been reported for the new Arge-based refinery, but is expected to be no less than 14-18%. The gas hourly space velocity requirements based on fresh feed for 88 and 94% $CO+H_2$ conversions are 663 hr^{-1} and 626 hr^{-1}, respectively. The catalyst life is not reported in the literature, but is expected to be short.

Shell is currently in the process of commercializing a new Fischer-Tropsch catalyst, apparently based on cobalt. The performance of this catalyst is not reported in the literature. Based on a Shell brochure, the C_1+C_2 selectivity appears to be between 2 and 3 wt.% [35].

Performance data at high conversion for some Shell cobalt catalysts are illustrated in UK Patent Application GB 2125062A [36] and in U.S. Patent 4,522,939 [37].

The best catalyst in the UK Patent Application, 25 Co:1.8 Zr:100 SiO_2, achieves 80% conversion at 600 gas hourly space velocity at 220°C, 30 atm, $2H_2$:1CO feed ratio in a fixed-bed reactor. This catalyst makes 10% methane + ethane, more than the Arge catalyst.

A catalyst in U.S. Patent 4,522,939, 25 Co:0.9 Zr:100 SiO_2 achieves 85% conversion at 1000 gas hourly space velocity at 220°C, 20 atm, and $2H_2$:1CO feed ratio in a fixed-bed reactor. The methane + ethane selectivity for this catalyst is not reported. However, from the reported 17% C_1-C_4 selectivity and from C_1+C_2/C_1-C_4 ratio for the catalyst in UK Patent Application 2125062A we estimate the methane + ethane selectivity in U.S. Patent 4,522,939 to be about 9%.

These results indicate that cobalt catalysts typically have high selectivity to methane + ethane at typical Fischer-Tropsch conditions. Alternatively, the catalyst may be operated at lower temperatures and lower H_2:CO ratios which would result in lower methane + ethane selectivities, but with a substantial activity penalty. However, examination of another Shell patent indicates that even at 195°C and $1H_2$:1CO feed ratio, the methane selectivity is still high: 4% [38]. It is not presently clear how Shell was able to lower the methane + ethane selectivity, ie., by a combination of optimizing the operating conditions or by developing a new catalyst.

Union Carbide, under Contract DE-AC22-84PC70028, developed a stable cobalt catalyst [39,40]. Union Carbide has not disclosed this catalyst's formulation.

This catalyst loses no more than 0.007% conversion/hour at 77% conversion, 260°C, 35 atm, $1.5H_2$:1CO feed ratio and 300 gas hourly space velocity in a Berty reactor. Assuming an activation energy of 25 Kcal/mole and a 16°C temperature increase between the beginning and end of a commercial run, a catalyst life of about 1.1 year is then estimated for Union Carbide's cobalt catalyst. However, under these conditions, this catalyst has a very high methane selectivity of 10% and C_2-C_4 selectivity of 11%.

Union Carbide was able to lower the methane selectivity of the cobalt catalyst to 3.6% by lowering the H_2:CO feed ratio to 1.0 at 240°C and 48% conversion, apparently in a fixed bed reactor. At this conversion level, however, the H_2:CO ratio at the reactor outlet became 0.5 or lower because the usage ratio was much higher than the feed ratio. The catalyst was then run for 300 hours. Deactivation rates under these conditions have not yet been reported.

Mobil, under Contracts DE-AC22-80PC30022 and DE-AC22-83PC60019, developed a precipitated iron catalyst [19,20]. During the best run, this catalyst was operated for 816 hours at about 80% CO+H_2 conversion, 245°C, 15 atm and 0.8 H_2:CO ratio in a slurry bubble column reactor. The run was shut down at the end of 816 hours due to settling of the catalyst in the reactor. The methane + ethane selectivity increased from 2.5% to 4.5% during the run.

2.2.3 Review of Literature Reports on Hydrocarbon Cutoff

In the late seventies and early eighties there have been a number of reports in the literature concerning the non-Anderson-Schulz-Flory synthesis of some hydrocarbons selectively via certain Fischer-Tropsch type catalysts [41,42]. Although some of the deviations from the Anderson-Schulz-Flory distribution that were observed were explained by experimental artifacts [42-44], three promising areas were identified. These were selective Fischer-Tropsch synthesis:

i. via control of catalyst geometry,

ii. via dual-functional catalysts [45],

iii. under transient conditions [46].

Control of the catalyst geometry seemed the most promising approach at the time. Some of the work done under this approach is summarized in Table 2-1 [36-41]. Three types of catalyst systems were identified:

i. Y-zeolite encaged ruthenium, iron or cobalt [47-49]

ii. Cobalt or ruthenium prepared on narrow-size-distribution-pore-structure-alumina or silica with small pores [50,51]

iii. Well-dispersed carbonyl-derived iron [52]

Ruthenium particles, 1.3 nm in size and encaged in the supercage of a LaY zeolite, did not produce, to any significant extent, hydrocarbons with carbon number greater than 3 [53] (Figure 2-2). For 2 nm particles in LaNaY zeolite, a cutoff carbon number of 6 was reported, with a high selectivity to carbon numbers 1 and 5. For 4 nm ruthenium particles stabilized in holes formed by hydrolysis of the NaY zeolite, the cutoff carbon number was reported as 11. At higher metal loadings, some of the ruthenium particles migrated to the exterior surface of the NaY zeolite and formed particles as large as 15 nm. With this broader particle size distribution, a broader product distribution was obtained,

Table 2-1

HYDROCARBON CUTOFF HYPOTHESIS
LITERATURE REPORTS

CATALYST SYSTEM		SPECIFIC CATALYSTS	CUTOFF CARBON NUMBER	POSSIBLE CAUSES OF CUTOFF		
				SMALL METAL PARTICLE SIZE	SMALL PORE SIZE	EXPERIMENTAL ARTIFACTS
ZEOLITE-ENCAGED-	Ru	20Å Ru 40Å Ru ON Y-ZEOLITE	C_6 C_{11}	✓ ✓	✓ ✓	✓
	Fe	25Å Fe ON Y-ZEOLITE	C_{11}	✓	✓	✓
	Co	ON CdA-ZEOLITE	SELECTIVE TO C_3	✓	✓	✓
SMALL PORE-STABILIZED-	Ru	>20Å PORES on SiO_2	C_{10}	✓	✓	✓
	Co	65Å PORES on Al_2O_3	C_{10}	✓	✓	✓
VERY WELL DISPERSED CARBONYL DERIVED	Fe	<6Å Fe ON Al_2O_3	C_4	✓		✓

Figure 2-2. Anderson-Schulz-Flory Distributions with Ru/Y-Zeolite Based on the Work by H. H. Nijs et al. [53]

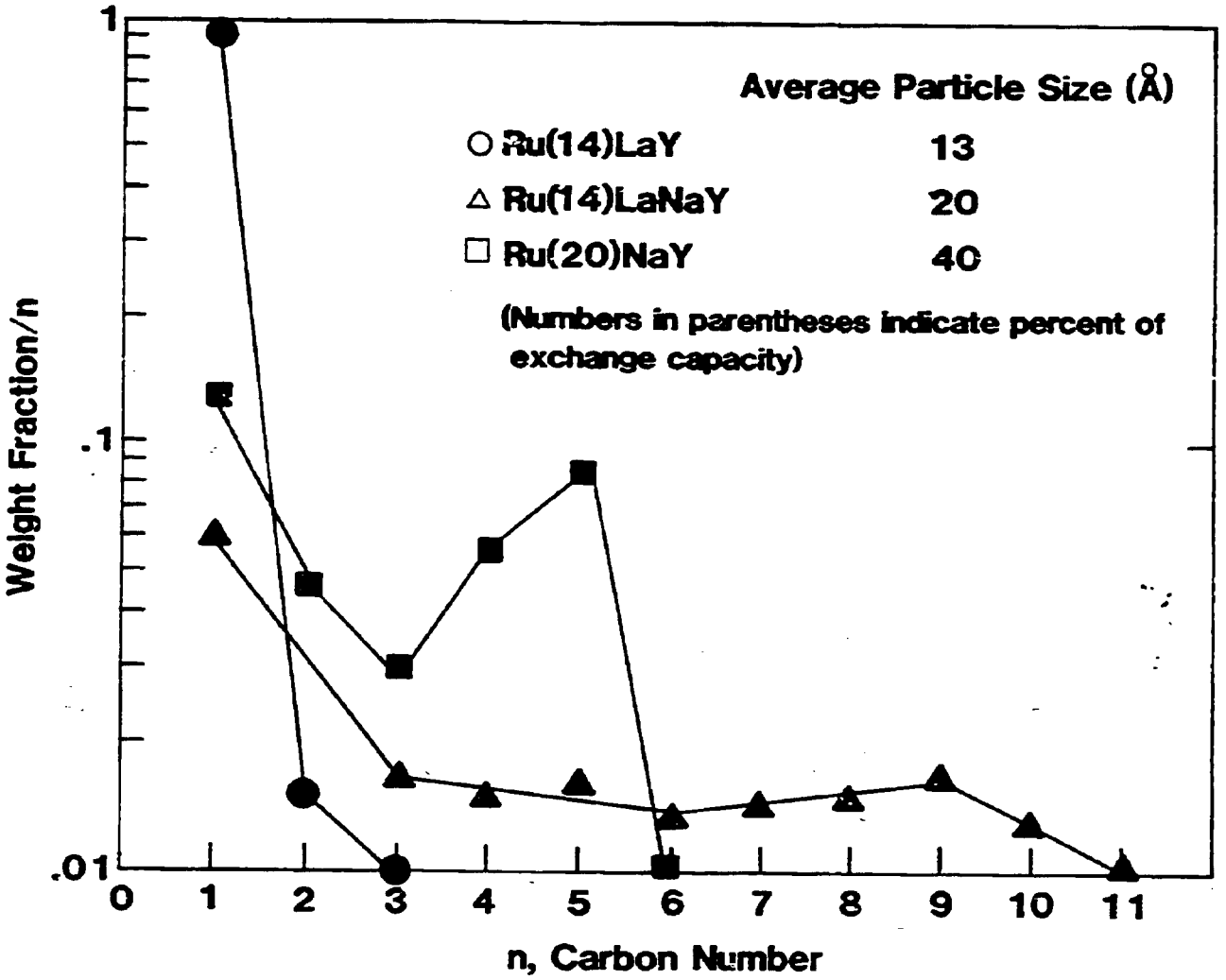

with 65 wt.% of the hydrocarbons in the C_{12+} range. It was reported that these deviations were not due to secondary reactions on the acidic sites or due to diffusional effects [36] but due to the catalyst geometry imposing a size limitation on the ruthenium particles.

Results obtained with Co/Al_2O_3 catalysts indicated that when the average pore diameter of the support was increased from 6.5 nm to 30 nm, the product distribution shifted toward higher hydrocarbons: from C_3-C_{10} to C_{14}-C_{20} [50].

Alumina-supported carbonyl-derived iron particles that had an initial size of <0.6 nm showed cutoff at a carbon number of 4 with a very high selectivity at C_2 (72.7 wt.%). These particles sintered with time and lost their selectivity to light hydrocarbons [52].

Evaluation of these literature reports indicated that a relatively small size for the active metal particle seemed to be common to each case. However, the possibility of experimental artifacts could not be ruled out, since analyses of used catalysts for condensed hydrocarbons were not reported in these works and also in some cases the conversion levels were very low.

2.2.4 Review of Literature Reports on Particle Size Effects with Supported Ruthenium Catalysts in Fischer-Tropsch Synthesis

Performance of supported ruthenium catalysts in Fischer-Tropsch synthesis has been shown to vary with metal particle size [54-58]. While it is generally agreed that with alumina-supported catalysts, the turnover frequency increases with increase in ruthenium metal particle size, the effect of ruthenium metal particle size on selectivity has not been clarified.

Kellner and Bell reported a slight decrease in the chain growth probability with increase in ruthenium metal dispersion on alumina at dispersions greater than 70%. Experiments were conducted at 206°C, 1 atm, $2H_2$:1CO and less than 2%

CO conversion [55]. Fukushima, *et al.* observed, by *in-situ* infrared spectroscopy at 230°C, 6 atm, and $2H_2$:1CO, higher chain length hydrocarbons on a 3% dispersed alumina-supported catalyst relative to a 24% dispersed catalyst [56]. King did not observe a correlation between chain growth probability and ruthenium metal dispersion on alumina at 250°C, 4 atm, $2H_2$:1CO and 2-18% CO conversion [57].

Kellner and Bell reported a rapid decrease in the olefin-to-paraffin ratio when ruthenium metal dispersions increased beyond 70% with alumina-supported catalysts [55]. Okuhara, *et al.* showed an opposite effect on experiments conducted at 200°C, 0.7 atm, $2H_2$:1CO and 10-30% conversion range. They reported that selectivity was independent of the conversion level [58]. King attributed the decrease in olefin-to-paraffin ratio with decrease in metal dispersion to an increase in the conversion level he observed in his experiments [57].

There has been no report on the effect of ruthenium metal particle size on the water gas shift reaction which occurs with alumina-supported catalysts. It is interesting to note that with zeolitic ruthenium prepared from the hexamine complex, the geometry of the faujasite supercage was found to be a prerequisite for low temperature water gas shift activity. The highest catalytic efficiency was reported when the supercage was occupied on the average by one Ru atom [22].

Decreases in percent metal exposed (measured by H_2 chemisorption) were reported with a 90% dispersed alumina-supported ruthenium catalyst during subsequent reaction rate measurements until a stable metal dispersion of 60% was obtained, implying a possible ruthenium metal particle size effect on ruthenium metal agglomeration [55].

2.2.5 Review of Micelle Literature

2.2.5.1 Principles of Micelle Formation

Two mutually insoluble phases such as water and oil can be made to disperse within each other by means of a surfactant which lowers the interfacial tension between them. An oil in water, o/w (normal), or a water in oil, w/o (reverse), micelle system is formed, depending upon whether the surfactant-water or the surfactant-oil interfacial energy is lowered to a greater extent [59]. Surfactants have been developed which can reduce the interfacial tension (energy/area) from 41 dyne/cm to 10^{-4}-10^{-5} dyne/cm [60]. Correspondingly, the interfacial area can increase from 10^{-4} m^2/g to 5×10^2 m^2/g, in the form of 100Å micelles (or droplets), without causing an increase in the total interfacial energy. The overall micelle formation process occurs spontaneously because the entropy change for dispersing the oil and water phases is positive [61].

Although the relative contribution of factors affecting micelle formation and the final equilibrium state of the micelle system are not well understood, micelle size can be controlled with the choice of the proper parameters. A co-surfactant, such as a medium chain length alcohol, can be added to the oil + water + surfactant mixture to lower the interfacial tension between the insoluble phases to an even greater extent and therefore allow a further decrease in micelle size. Suitable co-surfactants contemplated comprise compounds selected from straight chain aliphatic alcohols. However, the co-surfactant, which is usually more hydrophobic than the surfactant, can position itself between the surfactant molecules and cause an increase in the average distance between the polar head groups. This would create electrostatic repulsive forces, and possibly cause micelle growth by agglomeration. An electrolyte like NaCl has a similar effect by supplying counterions to the polar head groups of the

surfactant. The equilibrium size of an o/w (normal) micelle will, for instance, increases with the extent of the oil phase. Water has a similar effect on the size of w/o reverse micelles. Temperature, particularly for non-ionic surfactants, can also be used to vary the micelle size.

Kinetics of micellization are fast, i.e., the time constant of the slowest step usually being in the order of milliseconds. Thus, a narrow micelle size distribution around a thermodynamically determined value is quickly achieved upon mixing of the oil/surfactant/water mixture.

2.2.5.2 Reverse Micelle Procedure for Making Catalysts

A method has been reported for preparing metal particles in a narrow size distribution, around 3-5 nm, by using reverse micellar systems [62] (Figure 2-3). The method consists of dissolving a metal salt in the water core of the reverse micelle and of reducing the dissolved metal ion by hydrazine or hydrogen. Several reverse micellar systems were used for preparing colloidal solutions of Pt, Pd, Rh and Ir by this method. It was found that, in each case, the standard deviation of the average diameter of the reduced particles was ±10%.

Narrow size distributions were also reported for nickel boride particles prepared by a micelle method [63].

Recently, a proprietary reverse micelle procedure for preparing catalysts having metal particles of narrow size distribution was developed at UOP. Noble metal particles that were prepared on alumina were in the size range 2-3 nm, as detected by STEM. Larger particles, 3-4 nm were obtained by changing the preparation parameters. The narrow size distribution obtained by this procedure was also confirmed by x-ray diffraction measurements.

Figure 2-3

REVERSE MICELLE PROCEDURE FOR PREPARING SMALL METAL PARTICLES WITH A NARROW SIZE DISTRIBUTION

(P. Stenius et al., International Patent Application PLT/SE81/0091, 1981)

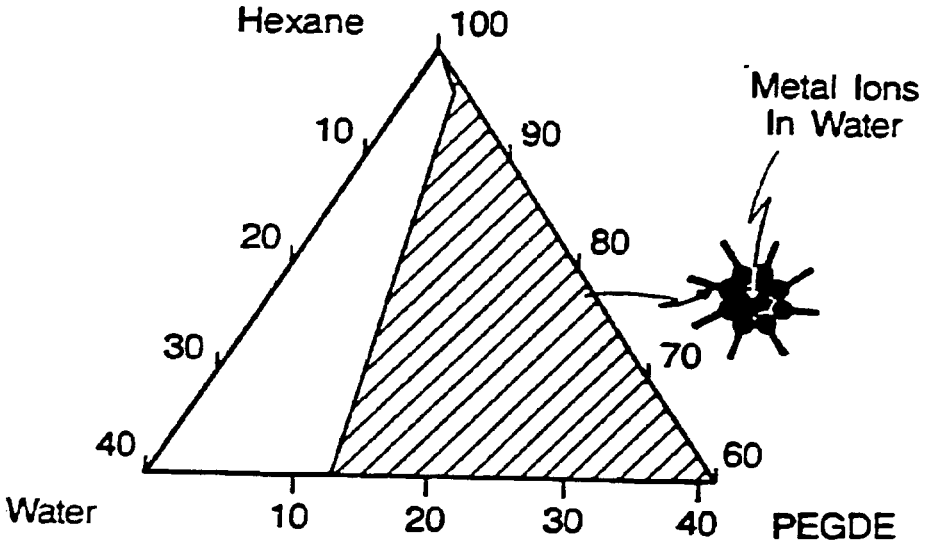

PEGDE: PENTAETHYLENE GLYCOL DODECYL ETHER

2.3 Research Approach

The research approach in this work consisted of three steps.

First, the experimental procedures were established. The experimental procedures included the application of the proprietary reverse micelle procedure to the preparation of supported ruthenium catalysts of controlled size, the application of gel permeation chromatography to the characterization of Fischer-Tropsch wax, the establishment of catalyst testing procedures using C-73-1-101 reference iron catalyst from United Catalysts Inc., the application of conventional aqueous impregnation to the preparation of highly dispersed ruthenium catalysts, and the application of EXAFS to characterization of ruthenium catalysts.

Second, the most promising catalyst developmental approach was selected. Both a non-Anderson-Schulz-Flory catalyst approach, which would result in a hydrocarbon cutoff at a carbon number of about 20, and an Anderson-Schulz-Flory catalyst approach with minimal selectivity to light ends were investigated. Then, the catalyst needs were identified for the most promising catalyst.

Third, the catalyst was improved by modifying the composition, followed by demonstration of the new catalyst. Then, the fresh and used modified catalysts were characterized.

2.4 Project Team

Dr. Hayim Abrevaya, from the Catalytic Process Technology Department, was the principal investigator for the project.

Mr. William M. Targos, from the Physical Chemistry and Surface Science Department, is the inventor of the proprietary reverse micelle technique, which was applied in this work to the preparation of supported ruthenium catalysts of controlled ruthenium particle size. Targos did the scanning transmission electron microscopy (STEM) work and made substantial contributions to the application of the reverse micelle technique to ruthenium catalysts.

Dr. Mehdi Akhbarnejad (Catalytic Science and Technology Department) made substantial contributions to the application of the reverse micelle technique to ruthenium catalysts.

Mr. Carl Lea (Engineering Development and Technology Department) designed the ruthenium catalyst finishing equipment and coordinated all catalyst finishing work. Mr. Robert G. Profitt, from the same department, was the technician assigned to the operation and maintenance of the Fischer-Tropsch pilot plant. Profitt, in this work, was assisted by a team of plant operators and shift supervisors.

Mr. Robert F. Swensen (Analytical Laboratories) developed the gel permeation chromatography technique that was used for analysis of Fischer-Tropsch wax.

Dr. Heinz Robota (Materials Science Department of Allied-Signal Engineered Materials Research Center) did the extended x-ray absorption fine structure (EXAFS) and x-ray diffraction (XRD) measurements and analyzed the data.

Mr. Frank Padrta (Physical Chemistry and Surface Science Department) developed techniques for characterization of coke by high resolution mass spectroscopy (HRMS), infrared spectroscopy and fluorescence analyses of solvent extracts from used catalysts. Padrta and Ms. Lillian Churchill, from the same department, did the measurements and analyzed the data.

Dr. Michelle Cohn (Physical Chemistry and Surface Science Department) did the gas adsorption measurements and analyzed the data.

Dr. Lorenz Bauer did the nuclear magnetic resonance (NMR) measurements and analyzed the data.

Ms. Sharon Varga and Dr. Jeff Donner did the x-ray photoelectron spectroscopy (XPS) measurements and summarized the data.

Dr. Pete M. Grill, who was from the same department, did the small angle x-ray scattering (SAXS) measurements and analyzed the data.

Dr. Chwu-Ching Jan did the CO adsorption measurements and analyzed the data.